Article:
Adamu, M and Kale, GM orcid.org/0000-0002-3021-5905 (2020) Novel MgHf4P6O24 as a Solid Electrolyte in Mg-Sensors. ECS Transactions, 98 (12). pp. 17-38. ISSN 1938-5862

https://doi.org/10.1149/09812.0017ecst

Novel $MgHf_4P_6O_{24}$ as a Solid Electrolyte in Mg-Sensors

Mohammed Adamu[1,*,y] and Girish M Kale[1]

[1]School of Chemical and Process Engineering, University of Leeds, Leeds LS2 9JT, United Kingdom.

[*]Electrochemical Society Member

[y]E-mail: mohammed.adamu@aol.com

ABSTRACT

In this paper, the electrochemical impedance analysis of $MgHf_4P_6O_{24}$ electroceramic oxide electrolyte on platinised pellets of 13mm diameter (Ø) and 3.8mm thickness depicts the electrical properties of Mg^{2+}-cation conducting species in the characterised solid-state electrolytes measured using the two-probe analysis at 182-764^oC, and from 100mHz to 32MHz, were evaluated. In this analysis, promising ionic conductivity of 4.52 x 10^{-4} Scm^{-1} for $MgHf_4P_6O_{24}$ electroceramic electrolyte was exhibited at 747^oC, thereby maintaining both materials and operational stability at $1000^oC \leq T/^oC \leq 1300$.

In addition to this, the design, fabrication and testing of solid-state Mg-sensors using the electrochemical method have been achieved. The novel high-temperature Mg-sensors were designed using the highly conducting Mg^{2+}-cation solid-state electrolyte by incorporating a biphasic powder mixture of $MgCr_2O_4$ + Cr_2O_3 solid-state reference electrode, which has shown promising trend after successfully sensing Mg dissolved in molten Al at 700±5^oC.

Keywords: synthesis, ionic conductivity, thermodynamic, transport number, electrochemical sensors, aluminium, magnesium

1. Introduction

Electroceramics such as magnesium zirconium phosphate and other phosphate solid-state electrolytes have been widely studied owing to their potential as solid electrolyte in electrochemical devices and thermodynamic measurements [1-7].

Recently, extensive attention has been assigned to the synthesis and characterisation of magnesium zirconium phosphate, $MgZr_4P_6O_{24}$, owing to their compositions and wide applications as ionic conductor in electrochemical devices. The various methods assigned to the synthesis of $MgZr_4P_6O_{24}$, such as solid-state method, sol-gel method, and hydrothermal method have yielded electrolytes with varied ionic conductivity.

The various intensive research interest in materials synthesis and characterisation however shows the benefit of knowing the behaviour of materials in operation. Today, various materials function in both ambient and high temperature environment, as such, appropriate materials are selected for certain application. Selecting materials for high temperature application requires operational stability of relevant materials properties as well as environmental suitability compared to applications at ambient temperatures. Temperature influences the stability of

functional materials in operation and the need to select materials suitable for different application is needed. Mg^{2+}-cation conducting behaviour of $MgZr_4P_6O_{24}$ solid-state electrolyte is believed to depend on the sol-gel synthesis technique [1, 2], it shows potential advantage of better homogeneity, better compositional control and lower processing temperature over the conventional solid-state method, which in this case accounts for a high percentage-relative density of the sintered sample pellets in ionic conductivity [1, 8]. Recently, we reported the Mg^{2+}-ion conducting behaviour of $MgZr_4P_6O_{24}$ solid-state electrolyte prepared using the sol-gel chemical synthesis method [1], with potential application as solid electrolyte in high-temperature electrochemical sensors and thermodynamic measurements.

In this study however, the ionic conductivity of $MgHf_4P_6O_{24}$ solid-state electrolyte was measured, and the design and fabricating of Mg-sensor probes using $MgHf_4P_6O_{24}$ as solid-state electrolyte and a biphasic powder mixture of $MgCr_2O_4 + Cr_2O_3$ as the reference electrode. The excellent ionic conductivity data of $MgHf_4P_6O_{24}$ solid-state electrolytes motivated the design and fabrication of solid-state Mg-sensors. In this study however, we report for the first time design and fabrication of novel high-temperature Mg-senor probes using the novel $MgHf_4P_6O_{24}$ solid-state electrolyte as Mg^{2+}-cation conductor. Sensing Mg in molten Al at 700±5°C was achieved by varying the Mg composition in molten Al, by alloying with 0.005-1.5 wt. % Mg. A biphasic powder equimolar mixture of $MgCr_2O_4 + Cr_2O_3$ open to ambient P_{O2} was used as Mg reference electrode in designing and fabricating the electrochemical Mg-sensors.

2. Materials and methods

2.1 Preparation and characterisation

All chemicals are analytical grade and used as received without further purification. Pure single phase $MgHf_4P_6O_{24}$ solid-state electrolytes were synthesised using sol-gel method to produce very fine powders; this is achieved through mixing on an atomic scale by combining aqueous solutions of soluble salts at a relatively low crystallisation temperature and, it produces compositions not always possible by solid-state fusion method. The stoichiometric amount of pure chemical solutions made from precursors; $Mg(NO_3)_2$, $HfCl_4$ and $NH_4H_2PO_4$, in aqueous form were mixed separately in adequate proportion for the synthesis of $MgHf_4P_6O_{24}$ solid-state electrolytes. The resulting dried xerogel powders were calcined at 900°C, pelletised and then sintered at 1300°C. The sintered pellets were characterised for their ionic conductivity and sensor evaluation. The electrochemical impedance spectroscopy measurement was achieved through the two-probe analysis method at 182-764°C temperature range, and from 100mHz to 32MHz frequency range.

2.2 Electrochemical impedance characterisation

For electrochemical impedance characterisation, the platinised pellets were prepared for impedance measurement by lightly grinding the two flat surfaces of the pellets sequentially on dried surfaces of silicon carbide (SiC) papers with grit size P400, P800, P1200, and P2500. Afterwards, geometric measurements on the sample pellets were achieved to determine the thickness and diameter of the solid-state electrolytes. Then, the sample pellets were platinised by applying platinum paste and cured at 800°C for 0.5h in order to provide a good adhesion

between platinum and solid-state electrolyte pellets and to also form contact electrode. The applied platinum provide good electrical contacts which also serves as a blocking electrode. The sample pellet was spring loaded in a quartz assembly rig placed inside a Faraday cage within horizontal Lenton LTF1200 tube furnace (Lenton Thermal Designs Ltd., Market Harborough, UK). A type-K thermocouple was inserted close to the sample pellet to subsequently monitor the actual temperature of the sample pellet at the point of impedance measurement. Furthermore, the actual temperature of the experiment was monitored and recorded through a plug and play temperature input device, the NI USB-TC01 to a LabVIEW interface (Business Park, Newbury, UK). The platinum wire clips were then connected to the Solartron SI1260 FRA impedance analyser which interfaced with a computer controlled by the software ZPlot (Scribner Associates, Inc. USA).

A schematic representation of the quartz assembly rig for impedance measurement is shown in Fig. 1. In this research however, the impedance analyser operates at a fixed applied voltage of 100mV and at an impedance furnace temperature range of $25 \leq T/\,^{o}C \leq 800$. In order to monitor the reversibility properties of the sample pellets, a temperature variance of 50 to 100^{o}C on decreasing and increasing temperature runs, respectively, depending on direction of measurements was applied. The impedance measurements were recorded after the measuring temperature had stabilised without temperature drift.

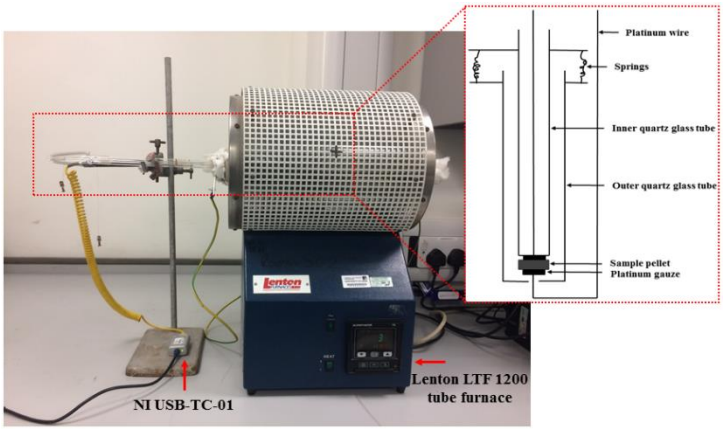

Fig. 1. Quartz assembly rig for impedance measurements in a Lenton LTF 1200 tube furnace

2.3 Sensor fabrication

The potentiometric sensors for high-temperature solid-state Mg-sensors characterised in this study for measuring concentration and determining the activity of Mg in liquid Al at 700±5^{o}C were designed and fabricated using high conducting ceramic solid-state electrolytes, a non-reactive annealed Fe-Cr alloy wire, Mo-rod counter electrode and a non-decomposing biphasic powder mixture of $MgCr_2O_4$+Cr_2O_3 reference electrodes.

2.3.1 Experimental setup

Sample pellets of $MgHf_4P_6O_{24}$ solid-state electrolytes was attached to an open end 50.8mm long alumina tubes using pure alumina refractory cement (Parkinson-Spencer Refractories Ltd., Halifax, United Kingdom) to form simple alumina probes. A 0.25mm thick annealed Fe-Cr alloy wire (Goodfellow, Cambridge) was coiled, inserted and rammed down into the bottom of the alumina tube along with a biphasic powder mixture of $MgCr_2O_4$+Cr_2O_3 which served as reference electrodes. The respective solid-state Mg-probes were extended by inserting them into a 120mm shock resistant SiAlON (Silicon Alumina Nitride) ceramic tubes, which were held firmly with alumina refractory cement to form bulk solid-state Mg-sensors, respectively, as shown in Fig. 2.

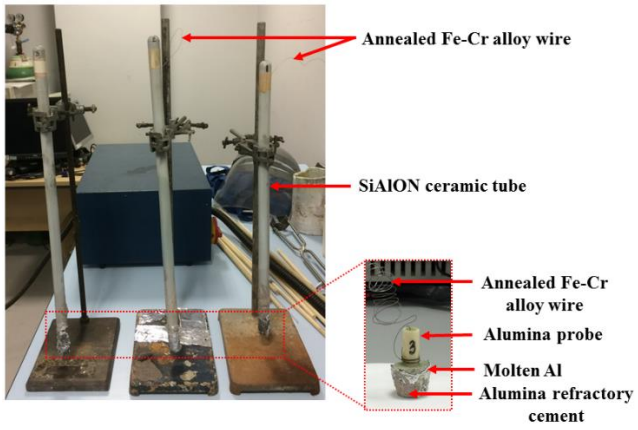

Fig. 2. Solid-state Mg-sensors. Insert is a simple Mg-sensor before coupling

3. Results and discussions

3.1 Thermal analysis and phase identification

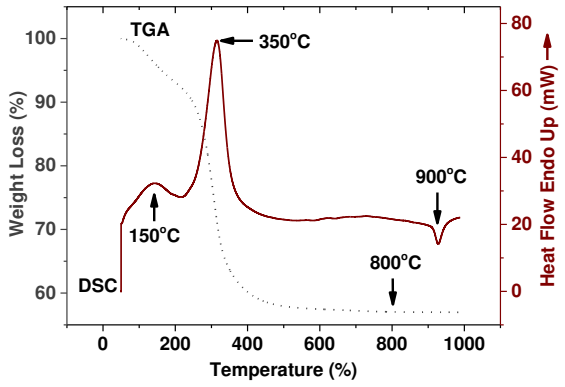

Fig. 3. TGA-DSC curves of $MgHf_4P_6O_{24}$ dried xerogel powders with scan rate of $10^oC\ min^{-1}$ in the air.

Thermal stability of the precursor xerogel of $MgHf_4P_6O_{24}$ solid-state electrolyte was analysed using simultaneous TGA-DSC. The main decomposition changes in the TGA profiles in Fig. 3 is presented in three different regions. The first region within 30-100°C corresponds to the removal of lattice H_2O. The weight loss in a temperature region of 150-500°C is due to the decomposition or oxidation of gelled inorganic precursor materials such as $Mg(NO_3)_2$, $HfCl_4$ and $NH_4H_2PO_4$. There was no further reduction in weight above 500±25°C for $MgHf_4P_6O_{24}$ xerogel powders. Similarly, the DSC profiles of $MgHf_4P_6O_{24}$ xerogel powders in the same figure shows two endothermic decomposition peaks at 150°C and 350°C, and an exothermic peak at 900°C. The inorganic precursor, $NH_4H_2PO_4$ decomposes into $(NH_4)_3H_2P_3O_{10}$ and H_2O molecules at temperature range of 140-170°C which could be responsible for the endothermic peak at 150°C. $Mg(NO_3)_2$ compound also decomposes into MgO, NO_2, and O_2 at a temperature above 300°C, this could be responsible for the endothermic peak at 350°C. The reactive oxide HfO_2 formed by the oxidation of $HfCl_4$ at 432°C yields $MgHf_4P_6O_{24}$ after stoichiometric reaction with MgO and P_2O_5 reactive oxides at 800°C - 900°C. Therefore, the exothermic peak observed at 900°C is for the formation of a single phase $MgHf_4P_6O_{24}$ with full crystallinity. The single phase $MgHf_4P_6O_{24}$ solid-state electrolyte started forming at 780°C as indicated on the TGA profile with absolute stability up to 900-1300°C range as was shown on the X-ray diffraction profile in Fig. 5. TGA-DSC measurements in this study was restricted to 1000°C because of the limitation of the equipment. Furthermore, it was noted that no further peak was observed on the DSC trace for $MgHf_4P_6O_{24}$ precursor at higher temperatures.

3.2 Relative density measurement

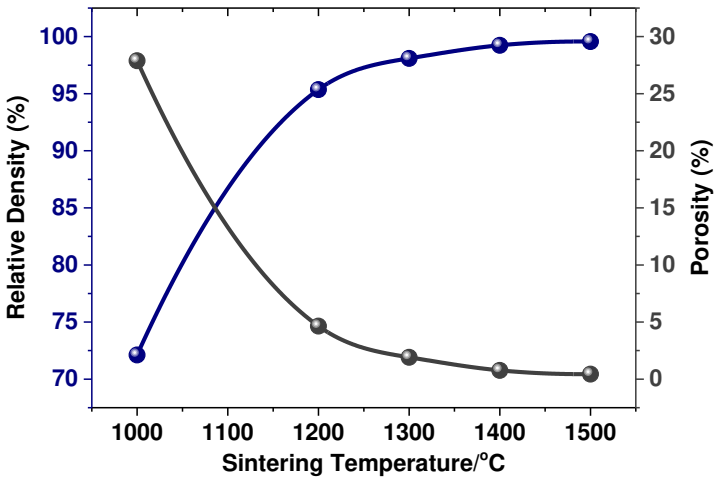

Fig. 4. Dependence of percentage-relative density and porosity of the sample pellets of $MgHf_4P_6O_{24}$ compound on sintering temperature

Solid-state $MgHf_4P_6O_{24}$ sample pellet presented in Fig. 4 shows that relative density increases continuously with sintering temperature, from 1000°C ≤ T ≤ 1500°C, with 24 h of annealing time. In Fig. 4, the sample pellet begins to show some densification (~95%) at temperature higher than 1100°C and exhibit an optimum density of about 98% at 1300°C for 24 h. Furthermore, the increment in density between 1300-1500°C is only ~1%, signifying that a

saturation point has been reached for the densification of $MgHf_4P_6O_{24}$ sample pellets. The porosity of ~2% was achieved at 1300°C which is considered good enough for the solid-state electrolyte sample pellets in sensor application. In this research, 1300°C sintering temperature at annealing time of 24 h was considered suitable for purpose of comparison and that since the difference in percentage-relative density is only ~1% from 1300-1500°C, a saturation point was already achieved at 1300°C. Using 1300°C as sintering temperature according to the density profile, a pure stable phase was also achieved for the characterised solid-state ceramic electrolytes.

Based on the thermal examination reported for $MgHf_4P_6O_{24}$ dried xerogel powders in Fig. 3, single phase $MgHf_4P_6O_{24}$ solid-state electrolyte was formed by calcining the dried xerogel powders at 800°C - 900°C. In addition, 1300°C was considered the sintering temperature of $MgHf_4P_6O_{24}$ solid-state electrolyte observed in the relative density shown in Fig. 4. Therefore, formation of $MgHf_4P_6O_{24}$ solid-state electrolyte presented in Fig. 5, shows single phase solid-state nanopowders calcined at 900°C and pellets sintered at 1300°C, with the majority peaks matched and indexed accordingly.

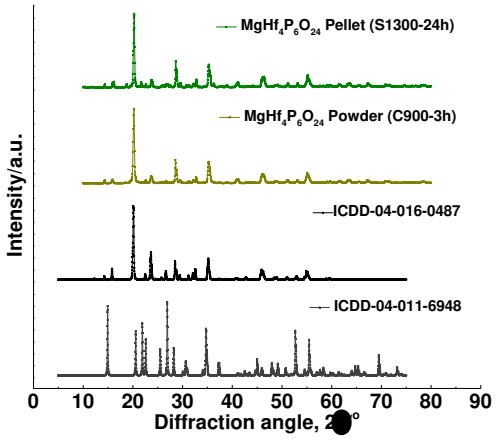

Fig. 5. Combined XRD peak profiles of $MgHf_4P_6O_{24}$ nanopowders calcined at 900°C and pellets sintered at 1300°C, respectively. All peaks were indexed to $Mg_{0.5}Zr_2(PO_4)_3$ [ICDD-04-016-0487], and $Zr_2(PO_4)_2O$ [ICDD-04-011-6948].

3.3 Impedance analysis

Electrochemical impedance analysis of a platinised $MgHf_4P_6O_{24}$ solid-state electrolyte is presented in Fig. 6. The impedance analysis of $MgHf_4P_6O_{24}$ solid-state electrolyte illustrated in Fig. 6 demonstrates the electrical properties of Mg^{2+}-cation conducting specie in $MgHf_4P_6O_{24}$ solid-state electrolyte. Fig. 6 further identifies the contribution from the grain interior, grain boundary and electrode-electrolyte interface in the high, intermediate and low frequency regions of the Nyquist plots for impedance analysis [9]. The impedance spectra measured in this study falls within the 182-747°C temperature and 100mHz-32MHz frequency range. In addition, the impedance spectra in Fig. 6(a) meanwhile shows a single slightly

depressed semicircle at higher-frequency followed immediately by the low-frequency spike inclined at angle of 45°. The appearance of such an inclined spike at low-frequencies therefore demonstrates the measured sample $MgHf_4P_6O_{24}$ as an ionic conductor similar to $MgZr_4P_6O_{24}$ sample pellets [10, 11]. The slightly depressed semicircle in Fig. 6 is attributed to the CPE parameter and it appears to suggest non-Debye type of relaxation behaviour [12] since the centre of the depressed semicircle is located below the axis, this electrochemical impedance behaviour is similar to those observed in other solid-state electrolytes [13]. Furthermore, real impedance, ReZ(Ω) obtained from intersection of the semicircle at a lower frequency with the x-axis, corresponds to the dc resistance. Also, the observed slightly depressed semicircle can result from the ionic migration in the bulk of solid-state electrolyte which is indicative of sintered sample pellets confirming the absence of grain boundary effects. Meanwhile, inclined spike in the low-frequency region may be attributed to the polarisation effect at the electrode-electrolyte interface [14], which is similar to the outcome of $MgZr_4P_6O_{24}$ impedance analysis [1]. The border frequency f_b in Fig. 6 corresponds to 6.38kHz, 1.60kHz and 2.02kHz for the $MgHf_4P_6O_{24}$ solid-state electrolyte at 273°C, 690°C and 747°C, respectively.

Electric modulus in Fig. 6(a) and Fig. 6(b) was relied upon to illustrate relaxation dynamics of the ionic species. Further, variations of imaginary component (M''/C_o) as a function of frequency (ω) at different temperatures show clearly the resolved peaks at unique peak frequencies, with the peaks displaying a tendency to shift towards a higher frequency region with increase in temperature. This behaviour suggests a conduction mechanism which is a thermally activated type of correlated hopping of Mg^{2+}-cations. Reproducibility mechanism is presented in Fig. 6(a) which shows no clear temperature profile deviation at 273-275°C.

As impedance temperature increases from 273°C in Fig. 6(a) to 690°C and then 747°C in Fig. 6(b), the depressed bulk semicircle gradually becomes smaller and, the inclined spike on the electrode-electrolyte interface gradually bent downward to become a depressed semicircle, this implies that as the bulk resistance R_b is decreasing the reversibility of charge migration at electrode-electrolyte interface is increasing [15]. Furthermore, the semicircles seen in Fig. 6(b) are not starting from the origin, implying there is a finite resistance R_s representing a lumped electrode-electrolyte interfacial resistance in series with a parallel combination of R_b and CPE_b representing constant phase element, CPE.

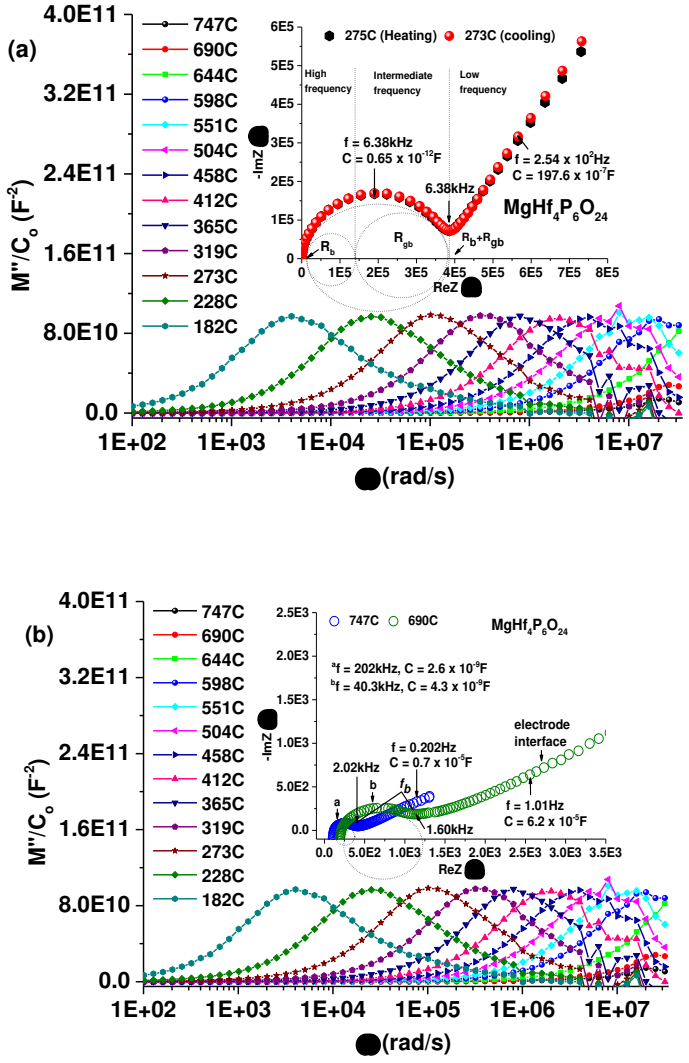

Fig. 6. Nyquist plots and electric modulus of $MgHf_4P_6O_{24}$ solid-state electrolyte at (a) 273-275°C (b) 690°C and 747°C temperatures in 100mHz-32MHz frequency range

The calculated value of the capacitance of the Nyquist plots of $MgHf_4P_6O_{24}$ solid-state electrolyte at different temperatures using frequency at the maximum point of both semicircles in Fig. 6(a) and Fig. 6(b) is illustrated in Table 1:

In using the relationship, $C = (2\pi fR)^{-1}$ where f and R are considered the frequency and resistance of the electroceramic circuit;

Table 1

Capacitance values and their possible interpretation

Solid-State Electrolyte	Frequency (Hz)	Resistance (Ω)	Capacitance (F)	Phenomenon Responsible [10]
$MgHf_4P_6O_{24}$ (273°C)	$6.38x10^3$	$3.85x10^5$	$0.65x10^{-12}$	bulk
45° electrode spike	$2.54x10^2$	$3.17x10^5$	$197.6x10^{-7}$	sample-electrode interface
$MgHf_4P_6O_{24}$ (690°C)	$40.3x10^3$	$9.18x10^2$	$4300x10^{-12}$	bulk
45° electrode spike	$0.101x10^1$	$2.54x10^3$	$6.2x10^{-5}$	sample-electrode interface
$MgHf_4P_6O_{24}$ (747°C)	$2.02x10^5$	$3.03x10^2$	$2600x10^{-12}$	bulk
45° electrode spike	$2.02x10^{-1}$	$11.47x10^2$	$0.7x10^{-5}$	sample-electrode interface

3.3.1 Temperature dependence of ionic conductivity

Fig. 7 describes the ionic conductivity of $MgHf_4P_6O_{24}$ solid-state electrolyte as a function of temperature. In this analysis, the ionic conductivity of $MgHf_4P_6O_{24}$ solid-state electrolyte was measured showing potential of being used interchangeably in structural and electrochemical applications. However, several details are outlined in Fig. 7; firstly, the linearity of the plots, which suggest there are no significant structural and phase changes noticed in the impedance temperature range. The activation energy, E_a which includes the energy of the formation and migration of ions in the solid-state electrolytes were determined from the gradient of Arrhenius plots by fitting the ionic conductivity data with Arrhenius equation presented in Eq. 1.

$$\sigma T = \sigma_o(T)\exp\left(-\frac{E_a}{kT}\right) \quad (1)$$

Ionic conduction has been found to be of thermally activated transport with different activation energy and ionic conductivity depending on the composition of electrolytes [16-18], which shows therefore, the ionic conductivity of samples in this study increases exponentially as the impedance temperatures increase. Moreso, the $MgHf_4P_6O_{24}$ solid-state electrolytes therefore exhibits an ionic conductivity of 4.52×10^{-4} Scm^{-1} at 747°C. Meanwhile, the bulk activation energy, E_a of $MgHf_4P_6O_{24}$ solid-state electrolyte shown in Figure 7 deduced from the slope of $\ln\sigma_{dc}T$ - $1000T^{-1}$ plots are 0.74±0.02eV. The E_a for $MgHf_4P_6O_{24}$ solid-state electrolyte in this study therefore signifies greater mobility of Mg^{2+}-cations, exhibiting an ionic conductivity at 747°C comparable with that earlier published [1]. In this study however, the conductivity data of $MgHf_4P_6O_{24}$ solid-state electrolyte in Fig. 7 was measured between 182-747°C and remains

chemically stable at higher temperatures compared to the $MgZr_4P_6O_{24}$ solid-state electrolytes, which transforms at sintering temperatures greater than 1300°C [1].

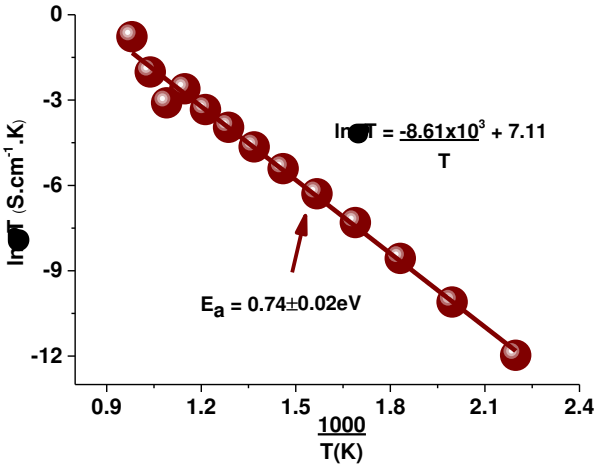

Fig. 7. Ionic conductivity of $MgHf_4P_6O_{24}$ solid-state electrolytes as a function of temperature

3.4 Testing of solid-state Mg-sensor

The electrochemical cell of solid-state Mg-sensors fabricated in this study is shown in Eq. 2:

$$(+)\ \text{air, Fe-Cr, } MgCr_2O_4+Cr_2O_3(s)/MgHf_4P_6O_{24}(s)/\text{Al-Mg(l), Mo } (-) \qquad (2)$$

The measured open circuit voltage of solid-state Mg-sensor at different Mg concentrations is presented in Eq. 3:

$$E/V\ (\pm 0.003) = 2.2013 + 0.0754 \text{Log} X_{Mg} \qquad (3)$$

The voltage generated across two dissimilar metal leads from the two electrodes is as shown; [Mo(+) - Fe-Cr(-)] at 700±5°C measured independently is -0.0093V. Therefore, the voltage of the cell in Eq. 2, corrected for thermo-emf measurement in this study is presented in Eq. 4:

$$E/V\ (\pm 0.003) = 2.1920 + 0.0754 \text{Log} X_{Mg} \qquad (4)$$

3.4.1 Analysis of solid-state Mg-sensor

Fig. 8 shows the response of Mg-sensor to changes in Mg concentration and its corresponding emf at a particular time, while holding the experimental temperature at 700±5°C. It further shows that while adding Mg-rod wrapped in Al-foil to a pure liquid Al at different intervals, the linear pattern signal of the Mg-sensor emf against the varied logarithmic composition of Mg demonstrates increasing emf of Mg-sensor to increasing concentration of Mg samples in liquid Al. It was however observed in this study that the solid-state Mg-sensor respond rapidly to Mg concentration on the first dipping, leading to fast equilibration at a shorter time which in most cases ensure an accurate amount of Mg concentration in the liquid Al.

The response sequence of Mg-sensor designed and fabricated using $MgZr_4P_6O_{24}$ as solid-state electrolyte and biphasic powder mixture of $MgCr_2O_4 + Cr_2O_3$ as reference electrode, varying the Mg concentration at 727±5°C has been published [2, 19]. The response sequences of solid-state Mg-sensor fabricated using $MgHf_4P_6O_{24}$ solid-state electrolyte in this study as presented in Fig. 7(a) shows the sensor emf increased to 1.92V with the addition of 0.005 wt.% Mg composition after the initial calibration and equilibration at a zero baseline. The addition of a further 0.05 wt.% Mg composition depicting an increment of about 40mV to achieve 1.96V after equilibration for 0.5h. Furthermore, sensor emf of 2.09V was achieved after the concentration was increased by a further addition of 0.5 wt.% Mg. The sensor emf then shows unstable progression with the addition of 1.0 and 1.5 wt.% Mg, with a stable emf progression of 2.10V, respectively. It therefore shows in this analysis that a voltage proportional to the logarithm of the Mg concentration with appropriate sensitivity was attained. However, it is clear that the solid-state Mg-sensor designed, fabricated and analysed in this study expresses a reasonable sensitivity sequence of the solid-state Mg-sensor which shows in the increasing voltage outlined in Table 2 for illustration purpose only:

Table 2

Mg-sensor sensitivity sequence with respect to Mg concentration

Mg (wt.%)	Voltage (V)
0.005	1.92
0.05	1.96
0.5	2.09
1.0	2.10
1.5	2.10

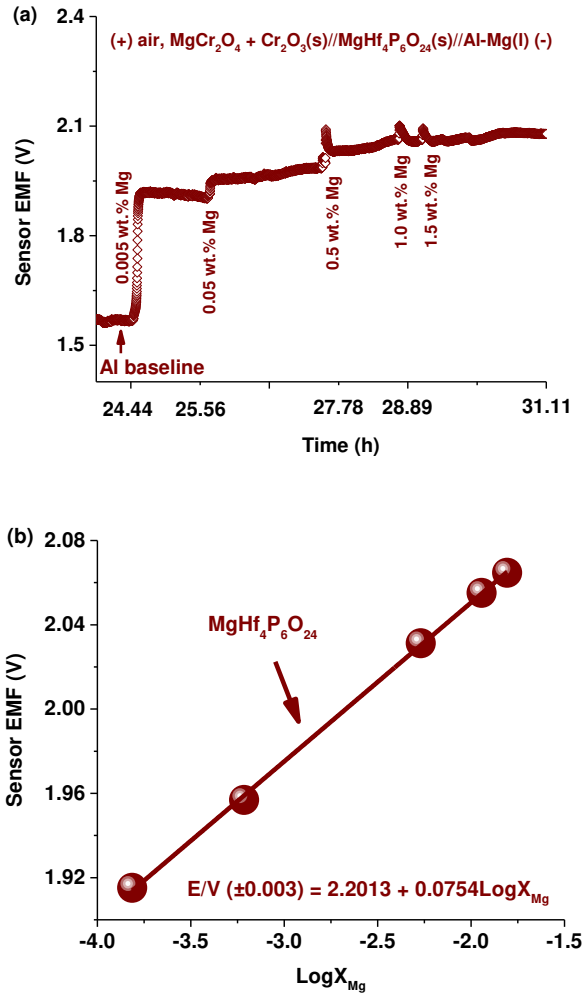

Fig. 7. Mg-sensor response as a function of Mg concentration in molten Al at 700±5°C, using (a) $MgHf_4P_6O_{24}$ solid-state electrolytes and biphasic mixture of $MgCr_2O_4$+Cr_2O_3 reference electrode in Mg-sensor fabrication, and (b) corresponding Mg-sensor emf variation using $MgHf_4P_6O_{24}$ solid-state electrolyte.

3.4.2 Transport number of Mg^{2+}-cation in $MgHf_4P_6O_{24}$ solid-state electrolyte

It is evident that during solid-state Mg-sensor testing in molten Al alloys, the activity of Mg is relatively high at the alloy electrode and very low at the ceramic electrode exposed to air.

The electrochemical reaction at the alloy electrode on the right-hand side of the cell is:

$$\{Mg\}_{Al(l)} \rightarrow Mg^{2+} + 2e^- \quad (5)$$

whereas, the electrochemical reaction at the reference electrode on the left-hand side is:

$$Mg^{2+} + 0.5O_2(g) + Cr_2O_3(cor) + 2e^- \rightarrow MgCr_2O_4(sp) \quad (6)$$

EMF (E/V) of the solid-state Mg-sensor defined in this study is presented as Eq. 7:

$$E\ (V) = -\frac{1}{nF}\int_{\mu_{Mg}^{ii}}^{\mu_{Mg}^{i}} t_{ion} d\mu_{Mg} \quad (7)$$

where F = Faraday constant in Coulombs mol^{-1}, n = 2 is the number of electrons participating in the electrode reactions, t_{ion} = transport number of the conducting species (Mg^{2+}), and μ_{Mg} = chemical potential of Mg defined as $RTlna_{Mg}$ where a_{Mg} = thermodynamic activity of Mg, the neutral form of the conducting species in the electrolyte. It is apparent from the polarity of the cell and emf response of the Mg-sensor that, the chemical potential of Mg at the reference electrode (μ^{ii}_{Mg}) is lower than that at the molten alloy sensing electrode (μ^{i}_{Mg}).

Assuming t_{Mg2+} in $MgHf_4P_6O_{24}$ is ≥ 0.99, emf of solid-state Mg-sensor can be calculated using thermodynamic activity of Mg in molten Al. The Gibbs energy of formation of $MgCr_2O_4$(sp) from its component binary oxides according to Jacob [20] is presented in Eq. 8 and Eq. 9:

$$MgO(rs) + Cr_2O_3(cor) = MgCr_2O_4(sp) \quad (8)$$

$$\Delta G^{o}_{f(ox)}\ (\pm 400)/Jmol^{-1} = -\ 45{,}200 + 5.36(T/K) \quad (9)$$

At 700°C (973K); $\Delta G^{o} = -39985 Jmol^{-1}$.

By combining this with the Gibbs energy of formation of MgO at the same temperature

$$Mg(l) + 0.5O_2(g) = MgO(s),\ \Delta G^{o}_{f} = -501401 Jmol^{-1} \quad (10)$$

The Gibbs energy change associated with the virtual cell reaction at 700°C is given by;

$$Mg(l) + Cr_2O_3(cor) + 0.5O_2(g) = MgCr_2O_4(sp),\ \Delta G^{o} = -541386 Jmol^{-1} \quad (11)$$

The estimated uncertainty in the value of Gibbs energy change for reaction (11) is 5 $Jmol^{-1}$. EMF of the Mg-sensor is related to the activity of Mg in molten Al by the relation;

$$-2FE = \Delta G = \Delta G^{o} + RTlna_{Mg} + 0.5RTlnp_{O2} \quad (12)$$

Thus, the theoretical emf of the sensor at 700°C can be calculated as;

$$E_{th}(\pm 0.026)/V = 2.7728 + 0.09653 loga_{Mg} \quad (13)$$

Aghdam and Soltanieh [21] measured the activity of Mg in molten Al using electrochemical cell with the eutectic mixture of $MgCl_2$-$CaCl_2$ as an electrolyte in a temperature range from 700 to 800°C and Mg composition from 0.07 to 12.1. The activity coefficient of Mg at 700°C for dilute alloys up to 1.4 atom % Mg can be expressed by the relation,

$$\log\gamma_{Mg} = -0.7624 + 23.183X_{Mg} \quad (14)$$

Expressing the activity of Mg in Eq. 13 as a product of mole fraction and activity coefficient, one obtains;

$$E_{th}(\pm 0.03)/V = 2.6992 + 2.2379X_{Mg} + 0.09653\log X_{Mg} \quad (15)$$

Fig. 8(a) shows the compared theoretical and measured emf, whereas, the average transport number is shown in Fig. 8(b). On the average however, the measured emf values are lower by ~0.359±0.022V. The average transport number at 700±5°C for Mg^{2+}-cations in $MgHf_4P_6O_{24}$ solid-state electrolyte over the range of chemical potential at the two electrodes are computed using the difference between experimental and theoretical emfs assuming that the electrodes are not polarised.

$$t_{ion} = \frac{E_{exp}}{E_{th}} \quad (16)$$

The average transport number for Mg^{2+}-cations in $MgHf_4P_6O_{24}$ solid electrolyte as a function of Mg concentration is 0.84±0.03 shown in Fig. 8(b).

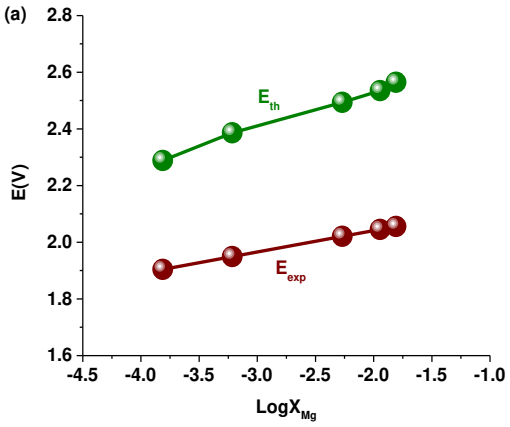

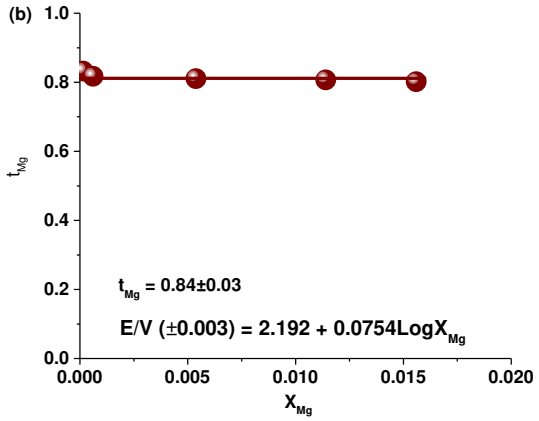

Fig. 8. The (a) relationship between measured emf of the Mg-sensor with the theoretical emf, and (b) variation of the average transport number of Mg^{2+}-cations in $MgHf_4P_6O_{24}$ at 700±5°C.

Conclusion

Based on TGA-DSC profiles, dried powders of $MgHf_4P_6O_{24}$ xerogels were calcined at 900°C to produce a single phase nanopowder of definite crystallinity. X-ray diffraction (xrd) further confirmed the formation of single phase nanopowders and pellets calcined and sintered at 900°C ≤ T/°C ≤ 1300. However, $MgHf_4P_6O_{24}$ solid-state electrolyte remain chemically stable at high-temperatures. Ionic conductivity of the novel $MgHf_4P_6O_{24}$ solid-state electrolyte is measured, characterised and reported for the first time in this study. The characterised solid-state electrolytes meanwhile attained stability in liquid Al at 700±5°C and were successfully used in the design and fabrication of high-temperature solid-state Mg-sensors for sensing Mg at varying concentration in molten Al.

Authors' information

*Email: mohammed.adamu@aol.com; Tel: 0044(0)7459749136

Orcid

Girish M Kale https://orcid.org/0000-0002-3021-5905

Mohammed Adamu https://orcid.org/0000-0002-5028-9370

Funding

The authors declare no competing financial interest.

Acknowledgements

The authors acknowledged the Tertiary Education Trust Fund (TETFund) for funding the PhD research student and the School of Chemical and Process Engineering, University of Leeds for the world class research infrastructure provided in support of this study.

References

(1) M. Adamu, G.M. Kale, Novel Sol-Gel Synthesis of $MgZr_4P_6O_{24}$ Composite Solid Electrolyte and Newer Insight into the Mg^{2+}-Ion Conducting Properties Using Impedance Spectroscopy. *J. Phys. Chem. C*. 120(32) (2016) 17909-17915.

(2) G.M. Kale, L. Wang, Y. Hong, High-Temperature Sensor for In-Line Monitoring of Mg and Li in Liquid Al Employing Ion-Conducting Ceramic Electrolytes. *Int. J. Appl. Ceram. Technol*. 1(2) (2004) 180-187.

(3) J.W. Fergus, Electrochemical sensors: Fundamentals, Key Materials, and Applications. Solid State Electrochemistry I: Fundamentals, Materials and their Applications. (2009) 427-491.

(4) V.I. Pet'kov, A.S. Shipilov, A.V. Markin, N.N. Smirnova, Thermodynamic Properties of Crystalline Magnesium Zirconium Phosphate. *J. Therm. Anal. Calorim.* 115(2) (2014) 1453-1463.

(5) G.M. Kale, K.T. Jacob, Thermodynamic Partial Properties of Na_2O in Nasicon Solid Solution, $Na_{1+x}Zr_2Si_xP_{3-x}O_{12}$. *J. Mater. Res.* 4(2) (1989) 417-422.

(6) G.M. Kale, A.J. Davidson, D.J. Fray, Investigation into an Improved Design of CO_2 Sensor. *Solid State Ionics.* 86-88 (1996), 1107-1110.

(7) S. Mudenda, G.M. Kale, Electrochemical Determination of Activity of Na_2O in $Na_2Ti_6O_{13}$-TiO_2 Two Phase System between 803-1000 K. *Electrochimica Acta.* 258 (2017) 1059-1063.

(8) M. Kakihana, Invited Review "Sol-Gel" Preparation of High Temperature Superconducting Oxides. *J. Sol-Gel Sci Technol*. 6(1) (1996) 7-55.

(9) J. Bauerle, Study of solid electrolyte polarization by a complex admittance method. *J. Phys. Chem. Solids.* 30(12) (1969) 2657-2670.

(10) J.T. Irvine, D.C. Sinclair, A.R. West, Electroceramics: characterisation by impedance spectroscopy. Adv. Mater. 2(3) (1990) 132-138.

(11) R.A. Huggins, Simple method to determine electronic and ionic components of the conductivity in mixed conductors a review. *Ionics.* 8(3-4) (2002) 300-313.

(12) J.R. MacDonald, "Impedance Spectroscopy-Emphasising Solid Materials and Synthesis," In: J.R. Macdonald, Ed., Theory, John Wiley and Sons Inc., New York, 1987, pp. 13, 77.

(13) B.V.R. Chowdari, R. Gopalakrishnan, Impedance and modulus spectroscopy of vitreous AgI-Ag_2O-P_2O_5 system. *Solid State Ionics.* 18 (1986) 483-487.

(14) P. Ferloni, A. Magistris, New materials for solid state electrochemistry. *J. Phys. IV France,* 4 (1994) C1-3-C1-15.

(15) Q.B. Bo, G.X. Sun, J. Meng, Preparation, structure and oxide ion conductivity in $Ce_{6-x}Y_xMoO_{15-\delta}$(x=0.1-1.4) solid solutions. *J. Phys. Chem. Solids.* 67(4) (2006) 732-737.

(16) M.G. Bellino, D.G. Lamas, N.E. Walsoe de Reca, A Mechanism for the Fast Ionic Transport in Nanostructured Oxide-Ion Solid Electrolyte. *Adv. Mater.* 18(22) (2006) 3005-3009.

(17) M. Prabu, S. Selvasekarapandian, A.R. Kulkarni, S. Karthikeyan, G. Hirankumar, C. Sanjeeviraja, Ionic Transport Properties of $LiCoPO_4$ Cathode Material. *Solid State Ionics.* 13(9) (2011) 1714-1718.

(18) A. Zuttel, Materials for hydrogen storage. *Mater. Today.* 6(9) (2003) 24-33.

(19) G.M. Kale, K.T. Jacob, L. Wang, Y. Hong, Solid-State Electrochemical Sensor For Monitoring Mg in Al Refining Process. *ECS Trans.* 1(13) (2006) 1-11.

(20) K.T. Jacob, Potentiometric determination of the Gibbs free energy of formation of cadmium and magnesium chromites. *J. Electrochem. Soc.* 124(12) (1977) 1827-1831.

(21) G.R.K. Aghdam, M. Soltanieh, Study of the Thermodynamic Properties of the Al-Mg Binary System Between 973-1073 K by the EMF Method. *Can. Metall. Quart.* 49(1) (2010) 39-45.